

Zero-modes of the QED Neuberger Dirac operator*

Bernd A. Berg^{a,b}, Urs M. Heller^c, Harald Markum^d, Rainer Pullirsch^d, and Wolfgang Sakuler^d

^aDepartment of Physics, The Florida State University, Tallahassee, FL 32306, USA

^bJohn von Neumann Institute for Computing, Forschungszentrum, D-52425 Jülich, Germany

^cSchool of Computational Science and Information Technology,
The Florida State University, Tallahassee, FL 32306, USA

^dAtominstytut, Technische Universität Wien, A-1040 Vienna, Austria

We consider $4d$ compact lattice QED in the quenched approximation. First, we briefly summarize the spectrum of the staggered Dirac operator and its connection with random matrix theory. Afterwards we present results for the low-lying eigenmodes of the Neuberger overlap-Dirac operator. In the strong coupling phase we find exact zero-modes. Subsequently we discuss possibly related topological excitations of the $U(1)$ lattice gauge theory.

1. Spectrum of the QED Dirac operator

The spectrum of the QCD Dirac operator

$$iD + im = \begin{pmatrix} im & T \\ T^\dagger & im \end{pmatrix} \quad \text{in a chiral basis} \quad (1)$$

is related to universality classes of random matrix theory (RMT), i.e. determined by the global symmetries of the QCD partition function, for a review see [1]. In RMT the matrix T in Eq. (1) is replaced by a random matrix with appropriate symmetries, generating the chiral orthogonal (chOE), unitary (chUE), and symplectic (chSE) ensemble, respectively. For $SU(2)$ and $SU(3)$ gauge groups numerous results exist confirming the expected relations.

We have investigated $4d$ $U(1)$ gauge theory described by the action $S\{U_l\} = \sum_p (1 - \cos \theta_p)$ with $U_l = U_{x,\mu} = \exp(i\theta_{x,\mu})$ and $\theta_p = \theta_{x,\mu} + \theta_{x+\hat{\mu},\nu} - \theta_{x+\hat{\nu},\mu} - \theta_{x,\nu}$ ($\nu \neq \mu$). At $\beta_c \approx 1.01$ $U(1)$ gauge theory undergoes a phase transition between a confinement phase with mass gap and monopole excitations for $\beta < \beta_c$ and the Coulomb phase for $\beta > \beta_c$. In the whole Coulomb phase the photon is massless and thus there ought to exist a

*This work was supported in part by the US Department of Energy under contract DE-FG02-97ER41022 and by the Fonds zur Förderung der wissenschaftlichen Forschung under project P14435-TPH. Based on a talk by BAB and a poster by RP.

continuum theory, as $V \rightarrow \infty$, everywhere.

We were interested in the relationship between $U(1)$ gauge theory and RMT across this phase transition. The Bohigas-Giannoni-Schmit conjecture [2] states that quantum systems whose classical counterparts are chaotic have spectral fluctuation properties, measured, e.g. by the nearest-neighbor spacing distribution $P(s)$ of unfolded eigenvalues, given by RMT, whereas systems whose classical counterparts are integrable obey a Poisson distribution, $P(s) = \exp(-s)$. With staggered fermions it was shown in Ref. [3] that the Bohigas-Giannoni-Schmit conjecture holds for lattice QED both in the confined phase (as for the $SU(2)$ and $SU(3)$ gauge groups) and also in the Coulomb phase, whereas free fermions yield the Poisson distribution. In Ref. [4] this investigation was continued with a study of the distribution of small eigenvalues in the confined phase. Excellent agreement was found for the conjecture that the microscopic spectral density

$$\rho_s(z) = \lim_{V \rightarrow \infty} \frac{1}{V\Sigma} \rho\left(\frac{z}{V\Sigma}\right) \quad (2)$$

is given by the result for the chUE of RMT, which also generates the Leutwyler-Smilga sum rules [1]. Here Σ is the modulus of the chiral condensate, which follows from the smallest non-zero eigenvalue via the Banks-Casher formula. The

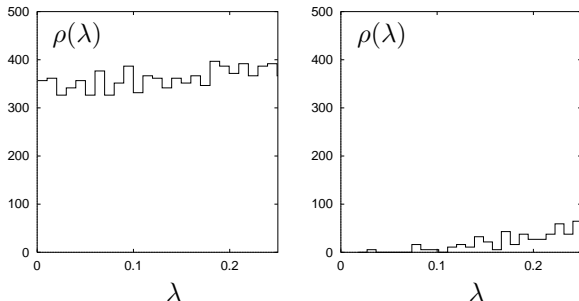


Figure 1. Density $\rho(\lambda)$ of small eigenvalues for the $8^3 \times 6$ lattice at $\beta = 0.9$ (left plot) and at $\beta = 1.1$ (right plot). A non-zero chiral condensate is supported in the confinement phase.

quasi zero-modes which are responsible for the chiral condensate build up when we cross from the Coulomb into the confined phase. For an $8^3 \times 6$ lattice [4], Fig. 1 compares on identical scales densities of the small eigenvalues at $\beta = 0.9$ (left plot) and at $\beta = 1.1$ (right plot), averaged over 20 configurations. The quasi zero-modes in the left plot are responsible for the non-zero chiral condensate $\Sigma > 0$ via the Banks-Casher formula, whereas no such quasi zero-modes are found in the Coulomb phase. For $4d$ SU(2) and SU(3) gauge theories a general interpretation is to link zero-modes to the existence of instantons. As there are no conventional instantons in $4d$ U(1) gauge theory (an analogous case exists in $3d$ QCD [5]), we [6] decided to study the physical origin of the U(1) quasi zero modes in more detail.

2. Exact zero-modes

Via the Atiyah-Singer index theorem the topological charge is mapped on the number of fermionic zero-modes of the Dirac operator. It is thus desirable to use a Dirac operator which retains chiral symmetry and exhibits exact zero-modes. Therefore, we employed in Ref. [6] the Neuberger overlap-Dirac operator [7,8]

$$D = \frac{1}{2} [1 + \gamma_5 \epsilon(H_w(m))] . \quad (3)$$

Here $\gamma_5 H_w(-m)$ is the usual Wilson-Dirac operator on the lattice and ϵ the sign function. The mass m has to be chosen to be positive and well

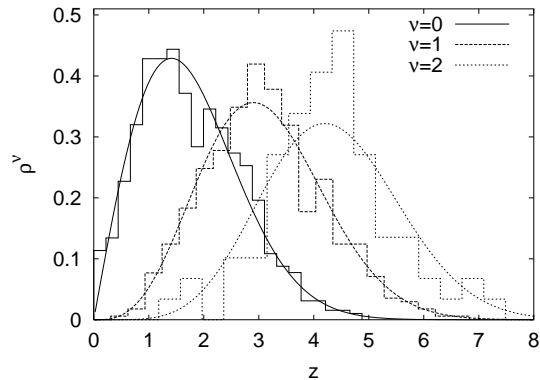


Figure 2. Exact RMT probability densities (5) for the lowest non-zero eigenvalues compared with histograms from our data.

above the critical mass for Wilson fermions but below the mass where the doublers become light on the lattice.

Our first question was whether the QED overlap-Dirac operator will exhibit exact zero-modes at all. To answer it, we have analyzed configurations on L^4 lattices at $\beta = 0.9$ in the confined phase and at $\beta = 1.1$ in the Coulomb phase. With an overrelaxation/heatbath algorithm we generated 500 configurations per lattice of linear size $L = 4, 6$ and 8 . After thermalization, the configurations were separated by 100 sweeps, with each sweep consisting of three overrelaxation updates of each link, followed by one heatbath update. On each configuration the lowest 12 eigenvalues of the overlap-Dirac operator (3) were calculated using the Ritz functional algorithm with the optimal rational approximation of Ref. [9] to $\epsilon(H_w(m))$ and m set to 2.3.

In the confined phase exact zero-modes of the operator (3) were indeed found. The highest degeneracy observed was $\nu = 3$. No zero-modes were found in the Coulomb phase. For each degeneracy ν , chiral RMT predicts the distribution of the lowest non-zero eigenvalue λ_{\min} in terms of the rescaled variable

$$z = \Sigma V \lambda_{\min} , \quad (4)$$

where V is the volume of the system and Σ the infinite volume value of the chiral condensate $\langle \bar{\psi}\psi \rangle$

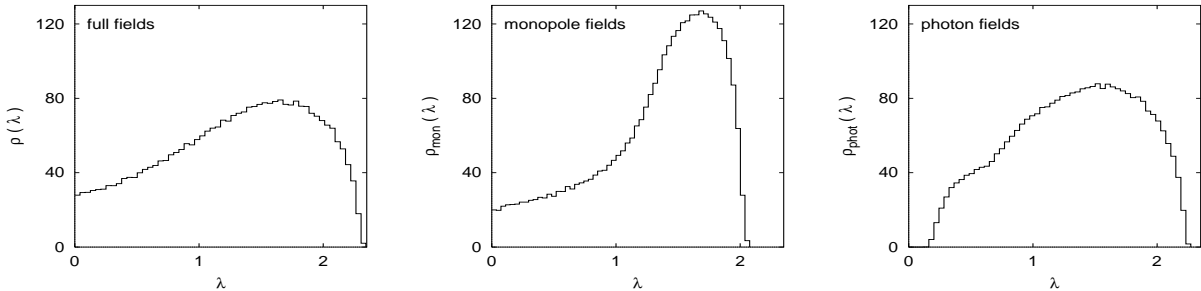


Figure 3. Decomposition of the spectrum $\rho(\lambda)$ (normalized to the number of eigenvalues) of the staggered Dirac operator into a monopole part $\rho_{\text{mon}}(\lambda)$ and a photon part $\rho_{\text{phot}}(\lambda)$, averaged over 500 configurations on a 4^4 lattice.

determined up to an overall wave function renormalization. For the U(1) gauge group the unitary ensemble applies and the RMT predictions for the $\nu = 0, 1, 2$ probability densities $\rho_{\text{min}}^{(\nu)}(z)$ are [1]

$$\rho_{\text{min}}^{(\nu)}(z) = \begin{cases} \frac{z}{2} e^{-\frac{z^2}{4}} (\nu = 0) \\ \frac{z}{2} I_2(z) e^{-\frac{z^2}{4}} (\nu = 1) \\ \frac{z}{2} [I_2(z)^2 - I_1(z)I_3(z)] e^{-\frac{z^2}{4}} (\nu = 2). \end{cases} \quad (5)$$

The chiral condensate is related to the expectation value of the smallest eigenvalue. For degeneracy ν we have

$$\Sigma = \Sigma^{(\nu)} = \frac{\langle z^{(\nu)} \rangle}{V \langle \lambda_{\text{min}}^{(\nu)} \rangle}, \quad (6)$$

where the result is supposed to be independent of ν and

$$\langle z^{(\nu)} \rangle = \int_0^\infty dz z \rho_{\text{min}}^{(\nu)}(z). \quad (7)$$

Using analytical and numerical integration the expectation values $\langle z^{(\nu)} \rangle$ are easily calculated. The values $\Sigma^{(\nu)}$ follow then from Eq. (6) and, for the various lattice sizes and ν 's, the results which we obtain from our data are consistent with one another.

Figure 2 displays the exact RMT probability densities $\rho_{\text{min}}^{(\nu)}$ of Eq. (5) and the corresponding histograms from our data. It shows that the histograms follow the shift of the RMT probability densities and their general shape. The high peak of the $\nu = 2$ histogram is interpreted as a statistical fluctuation due to the low statistics we have for this case.

3. Topological objects

The topological structure of the U(1) gauge theory is not as extensively studied as the non-Abelian case. Nevertheless, with torons [10], monopole solutions [11] and Dirac sheets [12] a number of topological objects are known for the U(1) gauge theory. All these topological configurations have in common with the zero-mode degeneracy that they are turned on at the phase transition from order (Coulomb) to disorder (confinement). However, in the confined phase we found no detailed correlation between any of the topological phenomena and the zero-mode degeneracy of the overlap-Dirac operator. Related to this may be that we found the zero-mode susceptibility to decrease, possibly approaching zero for $L \rightarrow \infty$ [6].

In contrast to these findings there is an interesting observation that ordered Dirac sheet configurations give rise to zero-modes of the overlap-Dirac operator, with the number of zero-modes being equal to the number of Dirac sheets [8,13]. One might understand this from the fact that a Dirac sheet is a $2d$ gauge configuration that contains unit topological charge in the $2d$ sense, kept constant in the two orthogonal directions.

To investigate possible correlations between the existence of zero-modes and topological objects further we have, following Refs. [14–16], factorized our gauge configurations into monopole and photon fields. The U(1) plaquette angles $\theta_{x,\mu\nu}$ are decomposed into the “physical” electromagnetic flux through the plaquette $\bar{\theta}_{x,\mu\nu}$ and a number

$m_{x,\mu\nu}$ of Dirac strings passing through the plaquette

$$\theta_{x,\mu\nu} = \bar{\theta}_{x,\mu\nu} + 2\pi m_{x,\mu\nu} , \quad (8)$$

where $\bar{\theta}_{x,\mu\nu} \in (-\pi, +\pi]$ and $m_{x,\mu\nu} \neq 0$ is called a Dirac plaquette. Monopole and photon fields are then defined in the following way

$$\theta_{x,\mu}^{\text{mon}} = -2\pi \sum_{x'} G_{x,x'} \partial'_{\nu} m_{x',\nu\mu} \quad (9)$$

$$\theta_{x,\mu}^{\text{phot}} = - \sum_{x'} G_{x,x'} \partial'_{\nu} \bar{\theta}_{x',\nu\mu} . \quad (10)$$

Here ∂' acts on x' , the quantities $m_{x,\mu\nu}$ and $\bar{\theta}_{x,\mu\nu}$ are defined in Eq. (8) and $G_{x,x'}$ is the lattice Coulomb propagator. One can show that $\tilde{\theta}_{x,\mu} \equiv \theta_{x,\mu}^{\text{mon}} + \theta_{x,\mu}^{\text{phot}}$ is up to a gauge transformation identical with the original $\theta_{x,\mu}$ defined by $U_{x,\mu} = \exp(i\theta_{x,\mu})$.

We found that both zero-modes and near zero-modes lie solely in the monopole part of the gauge field and are completely absent in the photonic field. Using periodic boundary conditions in space and anti-periodic boundary conditions in time [16], this was seen both for the overlap-Dirac operator and for the quasi zero-modes of the staggered Dirac operator. As an example we show in Fig. 3 the entire spectral density of the staggered Dirac operator in the original (full) gauge fields and in their monopole and photon part, respectively.

At the moment we are accumulating statistics to perform a decomposition into different topological sectors and to obtain an analogous analysis concerning topological objects as we did with the original U(1) field above [6]. It is of further interest to study space-time correlations between different topological objects. We pose the question of the existence of local correlations between the topological charge density and the monopole density. It is also desirable to calculate spatial correlations between the topological objects and the density $\psi^\dagger\psi(x)$ of the exact zero-modes of the overlap-Dirac operator.

4. Cooling

In non-Abelian theories it turned out that some cooling or smoothing procedure is unavoidable to

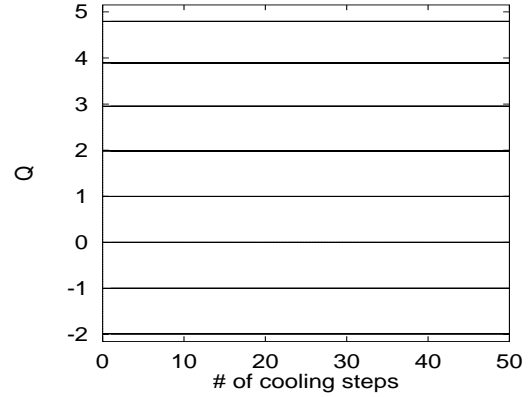


Figure 4. Topological charge of artificially constructed configurations on an 8^4 lattice.

gain integer-valued topological charges. For our Abelian case we studied the value Q obtained by integration of the topological density

$$Q = \int d^4x \frac{1}{32\pi^2} F_{\mu\nu}(x) \tilde{F}_{\mu\nu}(x) \quad (11)$$

using the hypercube definition and plaquette definition on the lattice [17]. In $4d$ U(1) theory with periodic boundary conditions one can construct an artificial configuration with integer topological charge Q [18]

$$\begin{aligned} U_1(x) &= \exp(i\omega_1 a x_2) \\ U_2(x) &= 1 \quad (x_2 = a, 2a, \dots, (N-1)a) \\ U_2(x) &= \exp(-i\omega_1 a N x_1) \quad (x_2 = Na) \\ U_3(x) &= \exp(i\omega_2 a x_4) \\ U_4(x) &= 1 \quad (x_4 = a, 2a, \dots, (N-1)a) \\ U_4(x) &= \exp(-i\omega_2 a N x_3) \quad (x_4 = Na), \end{aligned} \quad (12)$$

where N is the linear lattice extent, $\omega_i a^2 = \frac{2\pi n_i}{N^2}$, $n_i = \dots, -2, -1, 0, 1, 2, \dots$, and $Q = n_1 n_2$. These gauge fields consist of n_1 Dirac sheets in the 1-2 planes and n_2 Dirac sheets in the 3-4 planes. Such configurations possess nearly integer-valued Q 's on a finite lattice, as seen from Fig. 4, and the overlap-Dirac operator has Q exact zero-modes.

We have first heated and then cooled those smooth configurations in order to inspect whether they return to their original value of Q . In Fig. 5

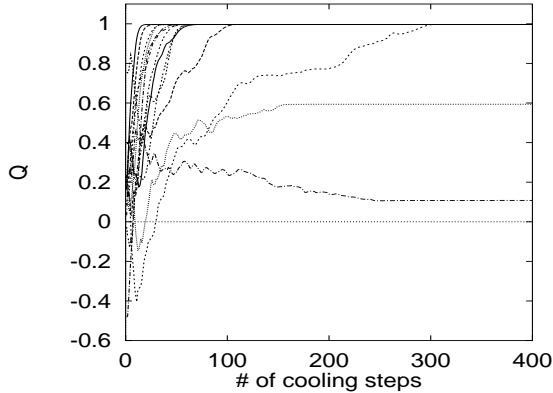


Figure 5. Cooling history of the topological charge of the $Q = 1$ configuration after increasing number of updates at $\beta = 0.9$. Integer topological charge is lost after $\lesssim 10$ updates.

we demonstrate the effect for the $Q = 1$ configuration which was updated several times with the Monte Carlo code at $\beta = 0.9$ before 400 cooling steps were applied. We employed a systematic cooling procedure by $U_\mu(x) \rightarrow VU_\mu(x)$, with $V = \frac{A^*}{|A|}$ and $A = \sum_{\eta=\pm 1} \sum_{\nu \neq \mu} U_\nu(x) S_{\mu\nu}^\eta(x)$. It turned out that the artificial configuration has a memory of $Q = 1$ for up to 10 Monte Carlo hits. When cooling equilibrium configurations from the $\beta = 0.9$ ensemble it never happened that they obtained an integer-valued topological charge, as depicted in Fig. 6.

5. Summary

- Exact zero-modes of the overlap-Dirac operator are observed in the confined phase of compact U(1) gauge theory.
- Agreement of the distribution of the smallest non-zero eigenvalue with predictions from random-matrix theory for fixed zero-mode degeneracy is found.
- No obvious correlations between toron charge, number of monopoles, number of Dirac sheets and the number of exact zero-modes is seen.
- Exact zero-modes survive in the monopole part

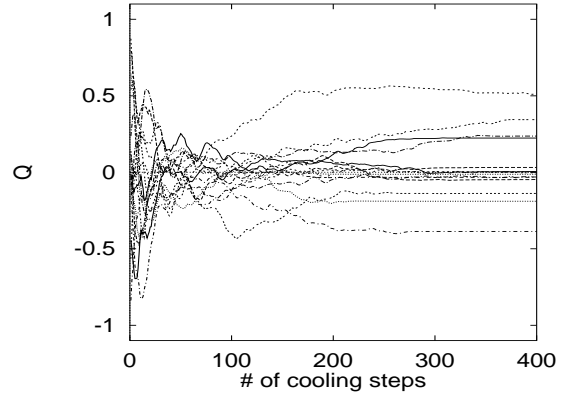


Figure 6. Cooling history of typical equilibrium configurations at $\beta = 0.9$. No integer topological charge is found.

of decomposed gauge field configurations, but not in the photon part.

- No equilibrium configurations with integer topological charge are found. Cooling does not lead to integer values for compact U(1) gauge theory.
- Only artificially constructed configurations have integer topological charge. Only for $\lesssim 10$ Monte Carlo updates can this charge be retained after cooling.
- Local spatial correlations between monopoles, topological charge density, and eigenfunctions of overlap-Dirac operator are analyzed currently to shed light on the confining mechanism of compact QED.

REFERENCES

1. J.J.M. Verbaarschot and T. Wettig, *Annu. Rev. Nucl. Part. Sci.* 50 (2000) 343.
2. O. Bohigas, M.-J. Giannoni, and C. Schmit, *Phys. Rev. Lett.* 52 (1984) 1.
3. B.A. Berg, H. Markum, and R. Pullirsch, *Phys. Rev. D* 59 (1999) 097504.
4. B.A. Berg, H. Markum, R. Pullirsch, and T. Wettig, *Phys. Rev. D* 63 (2000) 014504.

5. J.J.M. Verbaarschot and I. Zahed, Phys. Rev. Lett. 73 (1994) 2288.
6. B.A. Berg, U.M. Heller, H. Markum, R. Pulirsch, and W. Sakuler, Phys. Lett. B514 (2001) 97.
7. H. Neuberger, Phys. Lett. B417 (1998) 141.
8. R. Narayanan and H. Neuberger, Nucl. Phys. B 443 (1995) 305.
9. R.G. Edwards, U.M. Heller, and R. Narayanan, Nucl. Phys. B 540 (1999) 457.
10. A. Gonzalez-Arroyo, J. Jurkiewicz, and C.P. Korthals-Altes, NATO Advanced Study Institute, Series B: Physics 82 (1983) 339; G. 't Hooft, Nucl. Phys. B 153 (1979) 141.
11. A.M. Polyakov, Phys. Lett. 59B (1975) 82; S. Mandelstamm, Phys. Rep. 23 (1976) 245; G. 't Hooft, *High Energy Physics*, A. Zichichi (Ed.), Editrice Compositori, Bologna, 1976; T. Banks, R.J. Myerson, and J. Kogut, Nucl. Phys. B 129 (1977) 493; T.A. DeGrand and T. Toussaint, Phys. Rev. D 22 (1980) 2478.
12. V. Grösch, K. Jansen, J. Jersák, C.B. Lang, T. Neuhaus, and C. Rebbi, Phys. Lett. 162B (1985) 171.
13. T.-W. Chiu, Phys. Rev. D 60 (1999) 114510.
14. J.D. Stack and R.J. Wensley, Nucl. Phys. B 371 (1992) 597.
15. T. Suzuki, S. Kitahara, T. Okude, F. Shoji, K. Moroda, and O. Miyamura, Nucl. Phys. B (Proc. Suppl.) 47 (1996) 374.
16. T. Bielefeld, S. Hands, J.D. Stack, and R.J. Wensley, Phys. Lett. B416 (1998) 150.
17. P. di Vecchia, K. Fabricius, G.C. Rossi, and G. Veneziano, Nucl. Phys. B 192 (1981) 392; Phys. Lett. 108B (1982) 323.
18. J. Smit and J.C. Vink, Nucl. Phys. B 286 (1987) 485.